A Combined Nuclear Magnetic Resonance and X-ray Absorption Fine Structure Study on the Local Structures of Ge and Pb in $PbO-GeO_2$ Glasses and Their Relationships with Thermal Properties and Devitrification Products

P. Ghigna,*,† P. Mustarelli,† C. Tomasi,† E. Quartarone,† M. Scavini,‡ A. Speghini,§ and M. Bettinelli§

INSTM, Dipartimento di Chimica Fisica "M. Rolla", Università di Pavia, IENI-CNR sez. Pavia, V.le Taramelli 16, I-27100, Pavia, Italy, and INFM, Via Bassi 6, I-27100 Pavia, Italy, Dipartimento di Chimica Fisica ed Elettrochimica, Università di Milano, via C. Golgi 19, I-20133 Milano, Italy, and Dipartimento Scientifico e Tecnologico, Università di Verona and INSTM U.d. R. Verona, Ca'Vignal, Strada Le Grazie 15, I-37134 Verona, Italy

Received: May 17, 2002; In Final Form: July 22, 2002

Thermal and structural properties of xPbO/$(1-x)$$GeO_2$ glasses with $0.0 \leq x \leq 0.50$ were studied by means of differential scanning calorimetry (DSC), X-ray absorption fine structure (XAFS) on Pb L_{III} and Ge K edges, and ^{207}Pb solid-state NMR. Extended X-ray absorption fine structure (EXAFS) evidences on Ge indicated that most of the Ge is in tetrahedral coordination, which exhibits an increasing distortion toward higher distances for $x \geq 0.10$. Concerning the Pb environment, both EXAFS and NMR have shown that in all glasses most of the Pb ions are at the apex of a trigonal (PbO_3) or square (PbO_4) pyramid or both as in crystalline $PbGeO_3$. NMR has also shown that Pb enters as a modifier and, by increasing x, the PbO_3/PbO_4 ratio increases. The thermal behavior of the system can be interpreted by dividing the investigated compositional range into three regions: (i) $0 < x \leq 0.05$; (ii) $0.05 < x < 0.25$; (iii) $0.25 \leq x \leq 0.50$. In both region i and region ii, a nanoscale separation can be inferred because of the presence of nanocrystalline GeO_2 dispersed in the glassy matrix. In region iii, a complete miscibility was observed. The Pb environment and the nanoscale separation can clarify the complex devitrification processes found in this system.

1. Introduction

GeO_2-based glasses can be easily prepared and have been widely studied with various experimental techniques. The most easily prepared and the most extensively studied are glasses containing alkaline metal oxides.[1] In these glasses, there is a change in the Ge coordination from tetrahedral to octahedral with decreasing Ge content.[2] This change in the Ge coordination has been postulated to explain the maxima that are found in the trends of many physical properties of the glassy systems with composition, that is, the so-called germanate anomaly.[3] It also reflects the quite unusual polymorphism of pure GeO_2, which at room temperature can be found both in a quartz-like structure with tetrahedral coordination and in a rutile-like structure with a distorted octahedral coordination.

Among these systems, lead germanates display many chemical and physical properties that make them suitable for several technological applications. In this class of materials, glasses can be used in the field of optoelectronics as optical fibers,[4−5] whereas crystalline compounds are promising in view of their application as ferroelectric, pyroelectric, and electrooptic materials.[6−10] It can be noted, however, that lead germanate glasses are much less understood with respect to their structure than alkali germanates; in fact, there are just a few studies devoted to these aspects,[11−13] reporting conflicting conclusions. Therefore, a work devoted to the study of the local structure of xPbO/$(1-x)$$GeO_2$ glasses and to the thorough characterization regarding their thermal behavior and carried out with different structural probes is needed. Here, we present a joint NMR and X-ray absorption fine structure (XAFS) experimental inquiry in such a pseudobinary system on crystalline and glassy materials the thermal properties of which have been also thoroughly investigated. The aim of this work is twofold: (1) on one side, the clarification of the local chemical environment of Ge and Pb; (2) on the other side, the interpretation of the anomalous thermal behavior in this glassy system[14] and the complex devitrification processes[15] based on their structural properties. The two structural techniques, NMR and XAFS, can yield useful and complementary information.

In fact, on one hand, while high-resolution solid-state NMR has been proved to be a very powerful tool for the investigation of structure and local order in disordered solids, the applications to ^{207}Pb are still relatively scarce, chiefly because of low signal-to-noise ratio and the strong chemical shift interaction that gives very broad spectra. Only recently, reliable relationships among both isotropic and anisotropic chemical shifts and structures of Pb-containing oxide crystals have been established.[16] In particular, ionic salts display weak chemical shift anisotropy (CSA) patterns and large negative shifts, whereas covalent compounds with short Pb−O bond lengths (like lead oxides and silicates) are characterized by very strong CSA and more positive chemical shifts. Lead silicate[17] and lead oxychloride glasses[18] have been recently investigated in the frame of these ideas by means of modern NMR techniques.

On the other hand, it should be noted that ^{73}Ge is very difficult to investigate with NMR because of its high spin ($I = {}^9/_2$), and therefore, another structural probe is needed to get insights into the local structure of Ge in these systems. In this respect, XAFS can provide much benefit because the Ge K edge is easily within reach of almost every synchrotron radiation facility XAFS beamline. In addition, the Pb L_{III} edge is quite close in energy

† Università di Pavia, IENI-CNR sez. Pavia and INFM, unità di Pavia.
‡ Università di Milano.
§ Università di Verona and INSTM U.d. R. Verona.

10.1021/jp026133j CCC: $22.00
Published on Web 08/30/2002

TABLE 1: EXAFS Fitting Parameters for All of the Investigated Glasses and Crystals[a]

sample	x	D_{Pb-O} (Å)	σ^2_{Pb-O} (Å^2)	D_{Ge-O} (Å)	σ^2_{Ge-O} (Å^2)	D_{Ge-Ge} (Å)	σ^2_{Ge-Ge} (Å^2)
glass	0.50	2.31	7.0×10^{-3}	1.77	1.2×10^{-2}	3.23	7.0×10^{-3}
glass	0.35	2.27	1.8×10^{-2}	1.76	1.18×10^{-2}	3.21	3.6×10^{-3}
glass	0.25	2.28	1.6×10^{-2}	1.76	1.8×10^{-2}	3.16	1.1×10^{-3}
glass	0.20	2.30	1.4×10^{-2}	1.76	6.7×10^{-3}	3.22	3×10^{-3}
glass	0.10	2.27	1.9×10^{-2}	1.75	1.9×10^{-2}	3.19	4.1×10^{-3}
cryst $PbGeO_3$	0.50	2.28	1.6×10^{-2}	1.76	3.0×10^{-3}	3.18	6×10^{-3}
cryst $PbGe_3O_7$	0.25	2.38	1.8×10^{-2}	1.76	2.8×10^{-3}	3.25	3.3×10^{-3}
		2.68	2.4×10^{-2}				
		2.93	4.8×10^{-2}				
glass GeO_2	0.00			1.75	1.2×10^{-3}	3.20	4×10^{-3}
tetr GeO_2	0.00			1.85	5.8×10^{-3}		
				1.89	1.0×10^{-3}		
hex GeO_2	0.00			1.73	1.8×10^{-2}	3.17	

[a] Both Ge−K edge and Pb-L_{III} edge EXAFS parameters are shown. Errors should be estimated as ±1 on the last displayed digit.

and therefore can be collected with the same instrumental set up. Extended X-ray absorption fine structure (EXAFS) at the Pb L_{III} edge can be then used to extract structural parameters that can be compared or used as complementary information or both with respect to those obtained with ^{207}Pb NMR.

2. Experimental Section

Glassy samples of composition xPbO/$(1 - x)$$GeO_2$ with x ranging from 0.00 to 0.50 were prepared by melt-quenching. Appropriate amounts of analytical grade PbO (Aldrich, >99.9%) and GeO_2 (Aldrich, 99.998%) were mixed and melted in a platinum crucible in air. To pour melts having similar viscosity, the batches were held at 1100 °C ($0.30 \leq x \leq 0.50$), 1200 °C ($x = 0.20$ and 0.25), 1225 °C ($x = 0.15$), 1270 °C ($x = 0.10$), 1300 °C ($x = 0.05$), and 1500 °C ($x = 0.00$) for 1 h. All melts were quenched in air on a copper plate, but samples with $x = 0.05$ and $x = 0.50$ "water-quenched" by soaking the crucible containing the melt in cold water. The latter procedure was followed to prevent crystallization.

$PbGeO_3$ and $PbGe_3O_7$ crystalline samples were obtained by devitrification of the respective glasses at 660 °C for 360 h. Commercial quartz-like GeO_2 (Aldrich, 99.998%) and $PbSO_4$ (Aldrich, 99.999%) have been used as such; rutile-like GeO_2 was obtained by heating quartz-like GeO_2 for 700 h at 750 °C.

Differential scanning calorimetry (DSC) scans of all glassy samples were run at 10 °C/min under N_2 purge by means of a 2910 DSC and controlled by a Thermal Analyst 5000 (TA Instruments). The instrument was previously calibrated both in temperature and in enthalpy with standard indium.

XAFS spectra of selected xPbO/$(1 - x)$$GeO_2$ samples (see Table 1) were collected at liquid nitrogen temperature on both Ge K and Pb L_{III} edges at station BM 8 (GILDA, experiment no. 08-01-208) of the ESRF synchrotron radiation laboratory (Grenoble, France). The spectra were collected in transmission mode using ion chambers as detectors and a double crystal Si-(111) monochromator. For both the Ge K and Pb L_{III} edge measurements, an amount of sample appropriate to give an edge jump of about 1 in absorption coefficient was mixed with polyethylene and then pressed to pellet. For the X-ray absorption near edge structure (XANES) analysis, the spectra have been processed by subtracting the smooth preedge background fitted with a straight line and normalized to unit absorption at 1000 eV above the edge, where the EXAFS oscillations are not visible any more. The EXAFS analysis has been performed by means of the GNXAS package.[19−20]

^{207}Pb solid-state NMR spectra have been acquired on freshly ground samples with a AMX400WB spectrometer (Bruker, Germany) at the frequency of 83.7 MHz (magnetic field of 9.4 T). A 7 mm cross polarization magic angle spinning (CP-MAS) probe (Bruker) was used, but no differences were observed between the spectra acquired with sample rotation (up to 7 kHz) and the static ones, either in glasses or in the devitrified samples. MAS rotation improved the resolution only in the case of crystalline $PbSO_4$, which was used as a secondary chemical shift reference (−3613 ppm from $Pb(CH_3)_4$). The spectra were acquired both with single pulse (3 μs, corresponding to 30° tip angle) and Hahn echo sequences and averaged over 512 acquisitions. A spectral width of 1 MHz was used. When acquired with a single pulse, the free induction decays (FIDs) were left-shifted before the fast Fourier transform (FFT).

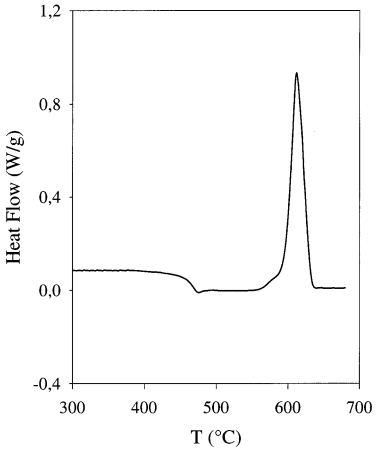

Figure 1. DSC thermogram of $0.25PbO/0.75GeO_2$ glass recorded at 10 °C/min.

3. Results

3.1. Thermal Behavior. Figure 1 shows the DSC thermogram of $x = 0.25$ as-quenched glass between room temperature and 650 °C. In this range, one can remark the deflection of the baseline at ∼460 °C corresponding to the glass-transition temperature, followed by an exothermic peak starting at ∼560 °C due to cold crystallization. All as-quenched glassy samples exhibit a similar behavior, despite their thermal features falling at different temperatures.

In Figure 2, the glass-transition temperature (T_g) of xPbO/$(1 - x)$$GeO_2$ glasses is plotted as a function of composition. Our data are in good agreement with those previously reported by Shelby et al.[14] but present a single glass-transition temperature for every examined sample. Pure GeO_2 exhibits a glass-transition temperature at about 525 °C, and small additions of PbO (<10 mol %) result in a sharp decrease of T_g. As larger amounts of PbO are added, T_g remains nearly constant around 460 °C, and for $x > 0.25$ an almost linear decrease of such a parameter with composition is observed.

3.2. XAFS Evidences. Figure 3 shows the XANES at the Ge K edge of the samples investigated in this work. The

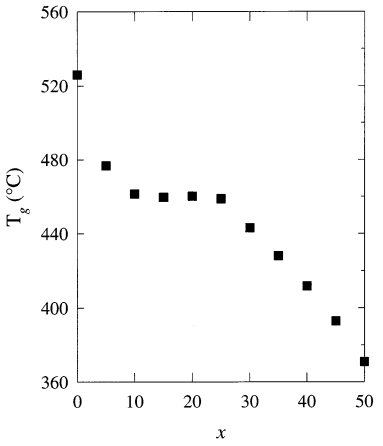

Figure 2. Glass-transition temperatures for all investigated compositions.

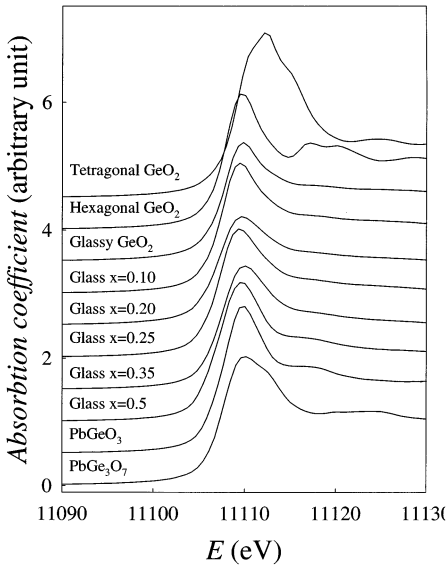

Figure 3. XANES spectra at the Ge K edge of the indicated glassy and crystal samples.

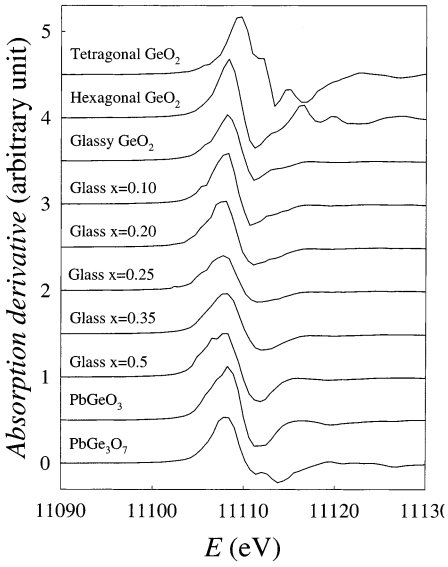

Figure 4. Derivatives of the XANES spectra of Figure 3.

corresponding derivatives are shown in Figure 4. It is clearly apparent that the overall XANES manifolds are very similar in all of the glassy samples and in hexagonal and vitreous GeO_2.

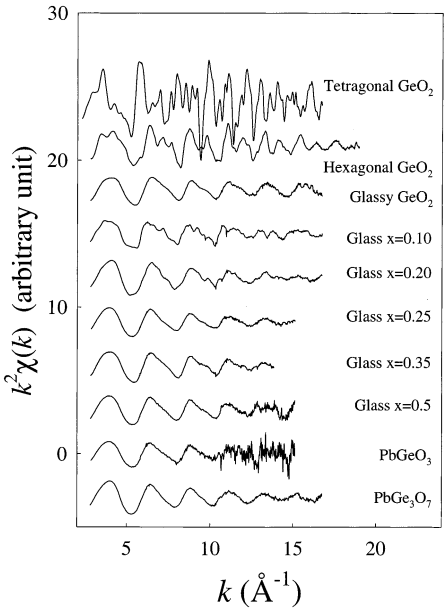

Figure 5. EXAFS spectra at the Ge K edge of the indicated glassy and crystal samples.

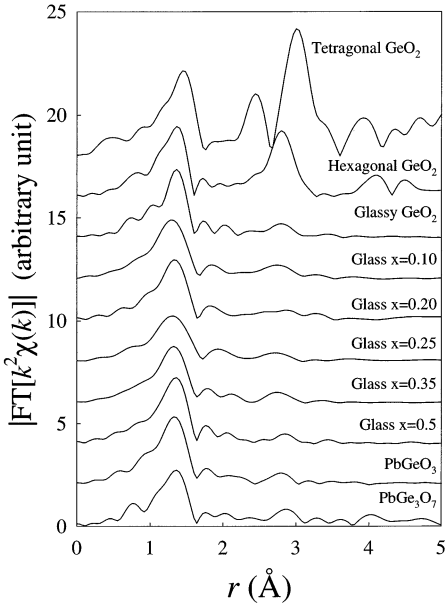

Figure 6. Fourier transforms (modulus) of the EXAFS spectra of Figure 5.

This is particularly evident in the derivative spectra. On the other hand, the XANES of tetragonal GeO_2 is quite different. Hexagonal GeO_2 has a quartz-like structure with Ge in tetrahedral coordination, while tetragonal GeO_2 has a rutile-like structure with Ge in a slightly distorted octahedral coordination; this explains both the differences in the XANES structures and the energy shift of the edges, as demonstrated by ab initio calculations.[21] The main conclusion that can be extracted from Figures 3 and 4 is that Ge coordination is quite similar in all of the glassy samples under investigation; in particular, it is quite apparent that Ge is mainly in tetrahedral coordination. Further insights on this point can be obtained by considering the EXAFS spectra at the Ge K edge, which are shown in Figure 5. The corresponding Fourier transforms are shown in Figure 6. When we recall that the EXAFS Fourier transform is related to the radial distribution function around the photoabsorber, it is apparent that for all of the samples the

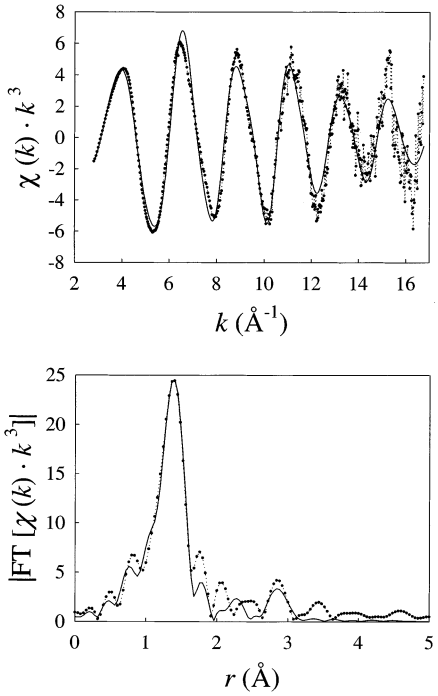

Figure 7. Ge K-edge (upper panel) EXAFS signal for glass x=0.50 and (lower panel) the corresponding Fourier transform. Dots and dotted lines represent experimental data; full line represents signal calculated according to the structural model described in text.

local chemical environment of Ge is quite close to that of hexagonal and glassy GeO_2. The most interesting feature in both glassy samples and crystalline $PbGeO_3$ and $PbGe_3O_7$ spectra is the presence of a next nearest neighbor shell at about 3 Å, which is reminiscent of that of hexagonal GeO_2 and therefore is attributed to Ge atoms belonging to the tetrahedral GeO_4 chains. This feature is less evident in both $x = 0.20$ and $x = 0.25$ glassy samples, probably because of the higher level of noise of the EXAFS spectra, which limits the available k range. In any case, all of the spectra have been analyzed with a two-shell model, using the shell radii, D_{Ge-O} and D_{Ge-Ge}, and the variance of the shell radius, σ^2_{Ge-O} and σ^2_{Ge-Ge}, as fitting parameters and keeping the coordination numbers fixed to 4 and 2, respectively, for the Ge−O and the Ge−Ge shells; this has been done to take into account the close similarity of the EXAFS spectra for all of the glassy xPbO/(1 − x)GeO_2 samples to those of hexagonal and glassy GeO_2. The results are summarized in Table 1. Figure 7 shows an example of the EXAFS fitting. The similarity of the Ge local chemical environment in all of the samples is emphasized by the closeness of the values in Table 1: Ge−O and Ge−Ge distances are found to be in the range 1.75−1.77 Å and 3.16−3.25 Å, respectively, for all samples, to be compared with the values of 1.75 and 3.20 Å, respectively, found for glassy GeO_2. Neither allowing the coordination numbers free to float nor adding further Ge−O or Ge−Pb distances led to a significant improvement in the quality of fit.

However, it should be noted that all that is reported above cannot be regarded as an irrefutable proof that there are no variations in the local chemical environment of Ge in the glassy samples with respect to each other and with respect to glassy GeO_2. Indeed, as pointed out by Ribeiro et al.,[11] the occurrence of octahedral Ge cannot be deduced by a straightforward EXAFS analysis.

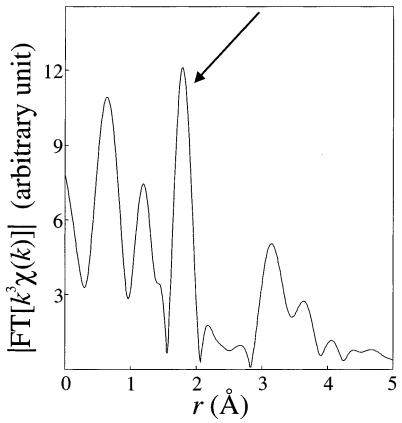

Figure 8. Fourier transform (modulus) of the difference EXAFS for the $x = 0.50$ composition, as described in text. The peak corresponding to the "new" coordination shell is indicated by the arrow.

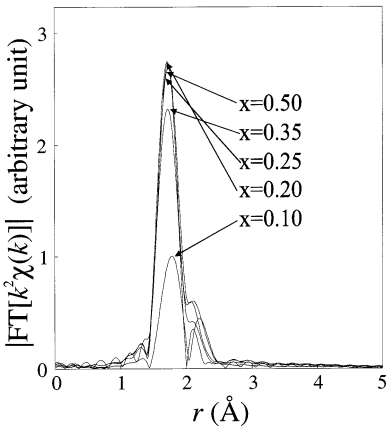

Figure 9. Fourier transform (modulus) of the difference EXAFS for the indicated compositions after Fourier filtering to extract the "new" coordination shell.

Actually, a "synthetic" spectrum assembled by averaging the spectra of tetragonal and hexagonal GeO_2 with 25:75 weights, respectively, can be fitted reasonably by the same model used for hexagonal GeO_2 with equivalent results.

To have a better insight on this point, the XAFS raw spectrum of glassy GeO_2 was subtracted from that of each glassy sample after normalization to unit edge jump. In the Fourier transforms of the difference spectra (see as an example Figure 8, in which the Fourier transform of the difference XAFS for the $x = 0.50$ composition is shown), a new coordination shell appears at nearly the same distance corresponding to the mean Ge−O distance that is found in tetragonal GeO_2 and therefore can be tentatively attributed to the presence of GeO_6 octahedra in glassy samples. This coordination shell can be isolated by Fourier filtering and therefore fitted using a GeO_6 cluster model. The fitted Ge−O distance is 1.85(3) Å for all of the samples; this value nicely compares with the equatorial Ge−O bond length equal to 1.85(1) Å resulting from our tetragonal GeO_2 EXAFS fitting and with the value of 1.89 Å determined by Umesaki et al.[12] from high-resolution neutron-diffraction measurements. Because of the difference procedure, it was difficult to obtain significant values for the coordination numbers. However, at least a comparative glance can be obtained by looking at Figure 9, which shows the Fourier transforms of all of the difference spectra after Fourier filtering. It is clearly apparent that the amount of GeO_6 octahedra increases rapidly by increasing Pb content for $x < 0.1$ and remains roughly constant for $x > 0.1$.

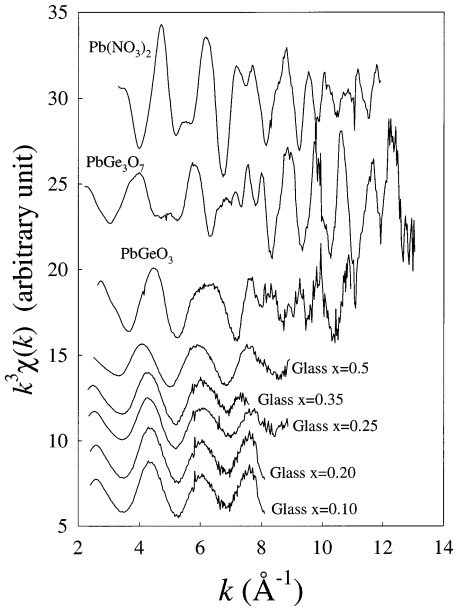

Figure 10. EXAFS spectra at the Pb L_{III} edge of the indicated glassy and crystal samples.

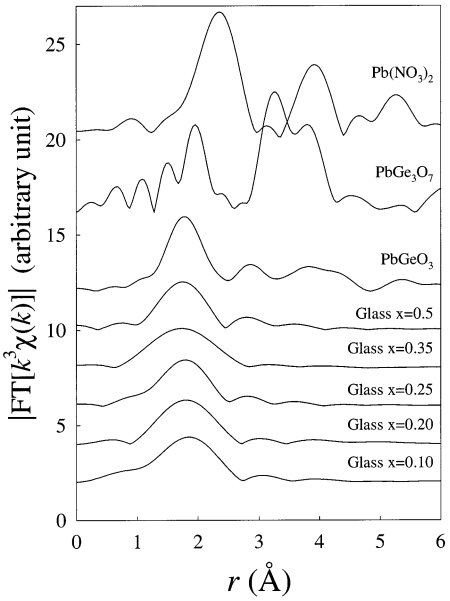

Figure 11. Fourier transforms (modulus) of the EXAFS spectra of Figure 10.

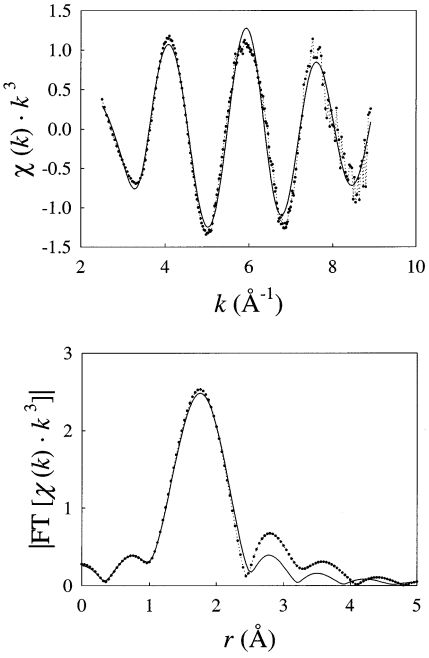

Figure 12. Pb L_{III} edge (upper panel) EXAFS signal for glass $x = 0.50$ and (lower panel) the corresponding Fourier transform. Dots and dotted lines represent the experimental data; full line represents the signal calculated according to the structural model described in text.

A convincing evidence that this is a real feature and it is not an artifact induced by the difference procedure is given by comparing the Fourier transforms of the difference spectra obtained from the spectrum of the $x = 0.5$ glassy sample and from the synthetic spectrum discussed above. The impressive similarity of these two Fourier transforms up to 4 Å nicely supports the validity of the difference procedure.

Strictly speaking, the above finding must be seen as proof of the presence of an anisotropic radial distribution function for Ge and not as an evidence of octahedrally coordinated Ge. In fact, the same procedure applied to crystalline $PbGeO_3$ and $PbGe_3O_7$ yielded an equivalent result with respect to those of glassy samples. In both crystals,[23,24] Ge coordination is highly dispersed: $PbGeO_3$ has three crystallographically nonequivalent tetrahedral Ge atoms with twelve Ge−O distances spread in the 1.68−1.78 Å range;[23] $PbGe_3O_7$ has also three nonequivalent Ge atoms with one Ge in trigonal bipyramid coordination (Ge−O mean distance 1.85 Å) and two Ge atoms in a distorted tetrahedral environment (Ge−O mean distance 1.74 Å).[24] Attempts to fit EXAFS spectra using an anisotropic radial distribution function (RDF) were indeed made by introducing a skewness term. Although large figures are obtained, their significance is doubtful because of (I) the small and variable *k* range among collected data and (II) strong correlations between the fitted parameters.

Taking into account the above warning, our results can be regarded as in agreement with that reported by Ribeiro et al.,[12] who described an increase of the Ge−O mean distance with Pb content and with that reported by Červinka et al.,[13] who could interpret their X-ray scattering data in terms of both a model consisting of corner-bound tetrahedra and a model consisting of a mixture of corner-bound tetrahedra and octahedra.

In all examined glasses, the local Pb environment detected by XAFS is very similar, as demonstrated by the Pb L_{III} edge EXAFS and their Fourier transforms shown in Figures 10 and 11, respectively. The EXAFS of crystalline $PbGeO_3$ is quite similar too. All of these spectra could be fitted with a single oxygen shell model; an example of the quality of the fits is shown in Figure 12. The fitted distances range from 2.27 to 2.30 Å for all of the glassy samples and crystalline $PbGeO_3$ (see Table 1). These values are quite close to that of the Pb−O distance found in red PbO (2.30 Å).[22] In this oxide, Pb is found in 4-fold coordination at the apex of a tetragonal pyramid. For this reason, in EXAFS fittings, the Pb coordination numbers have been kept fixed to 4. Allowing the coordination numbers free to float did not give reasonable results, because the fitted coordination numbers were always too much lower, ranging from 2 to 3. This may be due to the small *k* range available for the EXAFS, which reflects in a deep correlation between the coordination numbers and the σ^2 parameters. We therefore should point out explicitly that EXAFS in this case is quite inadequate for the determination of coordination numbers. In addition, it should be noticed that lead in square pyramidal and in trigonal pyramidal environments has almost the same Pb−O distances (~2.30 Å), and therefore, our EXAFS measurements

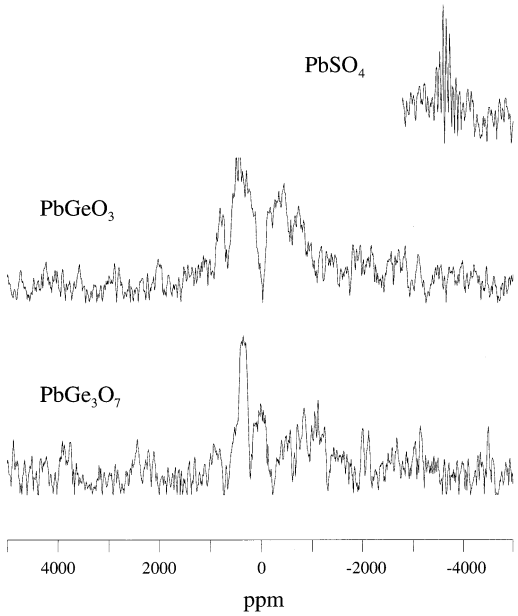

Figure 13. ^{207}Pb NMR spectra of crystalline $PbSO_4$ and of the devitrified samples $PbGeO_3$ and $PbGe_3O_7$.

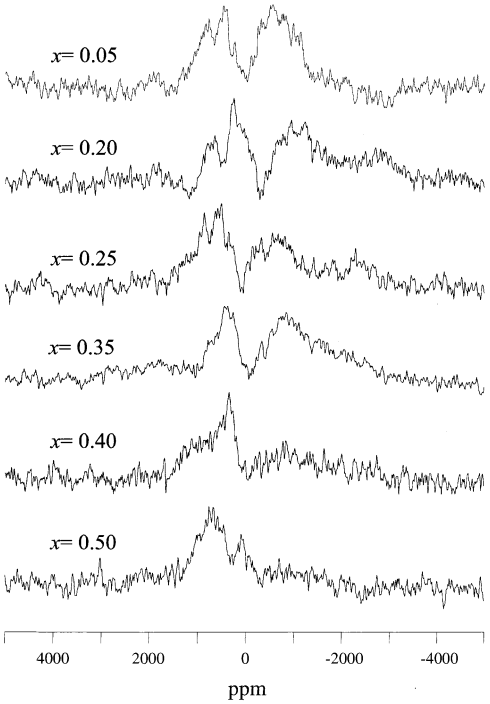

Figure 14. ^{207}Pb NMR spectra of glasses with $0.05 \leq x \leq 0.50$.

are unable to distinguish between these two coordinations. As a matter of fact, the EXAFS spectrum of crystalline $PbGeO_3$ could be fitted with a single Pb−O distance, although in this compound Pb is known to have both coordinations.[23]

The spectrum of crystalline $PbGe_3O_7$ is somewhat different and can be reasonably fitted by introducing at least three Pb−O distances (see Table 1) in agreement with crystallographic results.[24]

3.3. NMR Evidences. As long as XAFS evidences cannot detect significant differences for the Pb environment among the investigated glassy samples, information by the aid of ^{207}Pb NMR spectroscopy could be crucial. Figure 13 shows the spectra of crystalline $PbGeO_3$ and $PbGe_3O_7$ compared with that of commercial $PbSO_4$. Because the first two spectra show a broadening due to chemical shift interactions similar to that found in glassy samples, it is clear that the devitrification process has led to poor crystalline phases. This finding is in agreement with that found by Pb L_{III} edge X-ray absorption spectroscopy (XAS), along with previous X-ray powder diffraction (XRPD) patterns.[15]

The spectrum of $PbGeO_3$ (Figure 13) is characterized by two large and noisy features centered at ∼500 and approximately −400 ppm. As previously mentioned, the structure of crystalline $PbGeO_3$ contains three nonequivalent Pb, of which two are at the apex of a trigonal pyramid and the last one is at the apex of a square pyramid.[23] Following the literature[16] and on the basis of the relative intensities, we can assign the peak at low field (i.e., positive chemical shifts) to PbO_3 and the other one to PbO_4 groups. Similar peaks and assignments have been reported in covalent compounds such as silicates,[17] where Pb is three or four coordinated or both by oxygen ions in a pyramidal environment (Pb at the apex).

The spectrum of $PbGe_3O_7$ (Figure 13) is characterized by a relatively narrow peak centered at ∼420 ppm and by a large feature below −500 ppm. The structure of $PbGe_3O_7$ is well-known.[24] All of the Pb atoms are crystallographically equivalent and are coordinated by seven oxygen ions, three of which are at short distances (2.35, 2.43, and 2.48 Å, respectively) forming the basis of a trigonal pyramid. The isotropic chemical shift of Pb can be estimated using the empirical relationship proposed in ref 16 for the covalent compounds

$$\delta_{iso} = 2076.2 - 2180.2P$$

where P is a quantity related to the degree of s hybridization of the oxygen p orbitals and, in this case, to the number of Pb−O−Ge bonds. From the structure of $PbGe_3O_7$, we obtain $P \cong 0.88$, which gives $\delta_{iso} = 157$ ppm, in reasonable agreement with the observed value of 420 ppm. We therefore can assign this peak to the lead atoms in the unit cell of $PbGe_3O_7$, whereas the broad band at negative shifts is likely due to an impurity phase in which Pb nuclei experience longer Pb−O distances or higher coordination numbers with oxygen or both.

Figure 14 shows the ^{207}Pb NMR spectra of the glassy samples with $x = 0.05$, 0.20, 0.25, 0.35, 0.40, and 0.50. All of the spectral lines span over several thousands of ppm, as is generally observed in Pb-containing glasses.[17,18,25] The sample $x = 0.05$ displays two large features centered at 700 and −700 and a tail in the region below −1500 ppm. While a quantitative estimation of the spectrum is not possible because of the distortions due to uneven radio frequency (RF) irradiation, from a comparison with the spectrum of crystalline $PbGeO_3$, we can assign the two peaks to Pb at the apex of trigonal (PbO_3) and tetrahedral (PbO_4) pyramids, respectively. Here, the much greater peak widths reflect the intrinsic structural disorder of the glassy state. The tail at higher field (below −1500 ppm) can be assigned to Pb nuclei experiencing a more ionic environment (e.g., the ones connected to nonbridging oxygens) or a higher coordination (e.g., octahedral).[16]

The spectrum of the $x = 0.20$ sample is characterized by the same two features observed for sample $x = 0.05$ and by the formation of a relatively narrow peak around 400 ppm, that is, in the same spectral region of the one observed for crystalline $PbGe_3O_7$. Therefore, we can assign this peak to PbO_3 structural units with Pb−O−Ge bonds. We also stress that the intensity of the "tail" below −2000 ppm has increased.

Concerning the spectrum of the $x = 0.25$ sample, we chiefly observe that the feature at 400 ppm has disappeared. The spectrum of the $x = 0.35$ sample is characterized by relevant

shift to high field (from ~700 to ~400 ppm) of the PbO_3 peak in comparison with the sample $x = 0.25$. In addition, we observe that the intensity of the tail at approximately −2000 ppm does increase with respect to the PbO_4 peak.

Finally, the spectra of samples $x = 0.40$ and $x = 0.50$ are characterized by a progressive decrease of the high-field peak attributed to PbO_4 square pyramids. Moreover, we also note that the center-of-mass of the PbO_3 peak is progressively shifted to low fields. Both of these observations are in agreement with previously reported results on silicate glasses;[17] in particular, the last one can be related to the increase of the quantity of Pb−O−Pb covalent bonds.

4. Discussion

As mentioned above, all of our glassy samples exhibit a single glass-transition temperature (see Figure 2). The presence of a plateau for $0.05 < x < 0.25$ (see Figure 2) was previously reported in the literature and suggested the occurrence of an inhomogeneity in this compositional range.[14] By light scattering and electron microscopy experiments, Topping et al.[26] remarked the existence of a microstructure in glasses with $0.10 < x < 0.30$. This microstructure appeared to affect the dc resistivity and viscosity but not the thermal expansion coefficient. Later, Shelby[14] observed that the region of constant T_g in xPbO/$(1 - x)$$GeO_2$ glasses was very similar to the microstructure region reported by Topping but a little bit wider. As long as a similar behavior was exhibited by Ca, Sr, and Zn germanates, where opalescence makes phase separation well evident, it was concluded that in this compositional range lead germanate glasses were not homogeneous, despite the fact that no evidence of light scattering could be noted.

The possible inhomogeneity of our as-quenched samples was checked both by preliminary X-ray powder diffraction and scanning electron microscopy (SEM). XRPD patterns showed no Bragg peaks, excluding the presence of crystalline phases, whereas SEM micrographs revealed a homogeneous material, at least within the instrumental resolution (~1 μm). However, there are indications that pure GeO_2 itself has a certain tendency to nucleate. For this reason, Napolitano and Macedo, to produce GeO_2 seed-free glasses by fast quenching, kept the melt overnight at 1500 °C.[27] As described in the Experimental Section, our glassy GeO_2 was obtained by soaking the crucible previously kept at 1500 °C only for 1 h. As a matter of fact, a previous attempt, in which the melt was quenched down by pouring it into stainless steel moulds, yielded a partially crystalline material. For these reasons, we can tentatively explain the thermal behavior of our xPbO/$(1 - x)$$GeO_2$ glasses in terms of a structural inhomogeneity in the nanometer scale, that is, below the resolution of our SEM and XRPD techniques.

Let us now have a look at Figure 15, in which the heat capacity change at T_g is reported as a function of composition showing a maximum located around $x = 0.30$. In a work based on viscosity and thermal measurements, Lee et al.[28] found a similar behavior for the $x$$Na_2O$/$(1 - x)$$GeO_2$ glasses. Such a behavior was interpreted in terms of fragility of the glass, which changes with the Na_2O content, and is correlated to the germanate anomaly. In this case, a similar trend in T_g is expected, and it was indeed found for Na_2O−GeO_2 glasses.

On the other hand, for xPbO/$(1 - x)$$GeO_2$ glasses, the behavior of T_g shown in Figure 2 is completely different and needs a different model for its interpretation. Let us suppose that a significant part of our pure amorphous GeO_2 is nucleated and that the experimental ΔC_p value at T_g obtained by DSC is roughly proportional to the amount of the glassy phase present

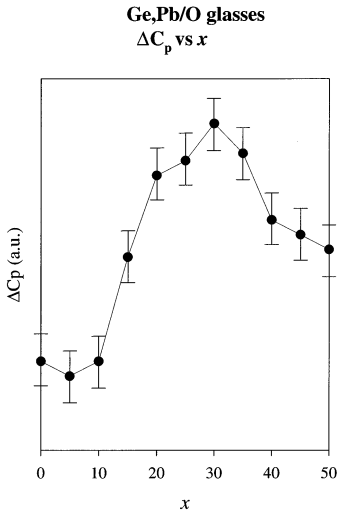

Figure 15. Heat capacity change at the glass-transition temperature for xPbO/$(1 - x)$$GeO_2$ glasses.

in the sample. Because of the size of nanocrystallites, no peaks could be detected by X-ray diffraction. It is expected[29] that lead oxide chiefly acts as a modifier; therefore, the addition of even small quantities of PbO will create nonbridging oxygens (NBOs) in the germania glassy network and, hence, lower the glass-transition temperature. In our case, it is reasonable that ΔC_p is more sensitive to the extent rather than the fragility of the glassy phase; hence, no significant changes of ΔC_p at T_g are foreseen. This seems to be the case for samples in the $0.00 \leq x \leq 0.10$ range (see Figure 2), in which a continuous decrease of the glass-transition temperature is observed, along with a nearly constant value of the heat capacity jump. For $x > 0.10$, the nucleation of GeO_2 gets more and more hindered. As a consequence, the fraction of glassy phase increases, as well as the extent of ΔC_p, while the glass composition keeps constant. In other words, lead oxide not only acts as a modifier by creating new NBOs in the GeO_2 network but also prevents its nucleation as long as a "limiting" or "more stable glass" with $x \approx 0.25$ is formed. This behavior is shown by samples within the $0.10 \leq x < 0.30$ range. Once the PbO content is high enough to almost completely encumber GeO_2 nucleation (i.e., when the sample is full glassy), further additions of lead oxide will increase the concentration of NBOs in a homogeneous glass and, consequently, will induce the decrease of both the glass-transition temperature and the heat capacity jump (see samples with $x \geq 0.30$).

This picture is supported by the ^{207}Pb NMR results, which allow us to divide the composition region that we explored into three parts, which can be referred to the role played by Pb in the glass and to a possible nanoscale phase separation: (i) $0 < x \leq 0.05$; (ii) $0.05 < x < 0.25$; (iii) $0.25 \leq x \leq 0.5$. In the following, we will discuss separately these three regions.

In region i, the spectrum of the sample $x = 0.05$ gives us the "fingerprint" of a covalent structure very similar (but for a higher disorder) to that of the crystalline $PbGeO_3$. On the other hand, the wide tail at negative chemical shifts points toward the formation of a fraction of more ionic bonds (e.g., Pb−NBO). This is in agreement with the decrease of T_g observed in Figure 2 and confirms that Pb chiefly acts as a modifier of the glassy matrix, as expected on the basis of the cation field strength model.[29]

In region ii, we can discuss the spectrum of $x = 0.20$ only. The narrow peak at ~400 ppm is likely due to some Pb atoms with a local coordination resembling that of $PbGe_3O_7$ (see Figure 13). We can so infer to have a phase separation giving (a) a

glass with constant T_g (460 °C, see Figure 2) and composition close to that of the $x = 0.25$ and (b) a crystalline GeO_2 nanophase. The nanocrystal−glass phase boundary can also act as an agent for heterogeneous nucleation of crystalline $PbGe_3O_7$, as demonstrated by our previous thermal measurements.[15]

Finally, for $x \geq 0.25$, the system can be seen again to be homogeneous as demonstrated by the disappearing of the peak at ~400 ppm. In this composition region, Pb acts again as a network modifier, as demonstrated by the lowering of the T_g and by the increasing of the Pb ionic fraction at high field.

Such a picture may account for the complex devitrification processes of $x PbO/(1 - x)GeO_2$ glasses[15] having, for the whole $0.00 < x < 0.50$ range, a strong tendency to crystallize first as metastable $PbGe_4O_9$. In the absence of nucleating agents as in region ii, the thermodynamically stable phase $PbGe_3O_7$ is formed only after prolonged firing at high temperature (e.g., 360 h at 660 °C).[15] The differences in the Pb environment of glasses and $PbGe_3O_7$ crystalline phase (see Figures 10 and 11) may justify the difficulty to reach equilibrium.

Unfortunately, as previously mentioned, Pb L_{III} edge XAFS cannot detect any difference in the local Pb environment of glasses; this can be attributed to (a) the high sensitivity of XAFS on atomic correlations, resulting in a lack of sensitivity on barely correlated phases, (b) the narrow *k*-range in which EXAFS oscillations are observed and the consequent low sensitivity toward next nearest neighbors, and (c) the closeness in the Pb−O distances when Pb is in a trigonal pyramidal or square pyramidal environment. It should be noted that also X-ray scattering experiments carried out by Červinka et al.[13] could detect a single Pb−O coordination sphere at about 2.43 Å, which was attributed to the presence of PbO_4 units. In this context, techniques such as NMR, probing local electric fields, can be regarded as more sensitive with respect to both XAFS and X-ray scattering, which sample pair distribution function (PDF).

On the contrary, the Ge K edge XAFS results are much more instructive. In particular, it has been shown that in all of the glasses of regions ii and iii the Ge coordination is increasingly distorted toward high distances.

In region ii in case of glass homogeneity, this increase with *x* should modify the structure of the glassy phase; hence, a change in T_g would be expected. This is in contrast with experimental results of Figure 2. On the contrary, under the hypothesis of nanoscale phase separation, such an increase could be ascribed to the increase of the amount of the glassy phase with $x \approx 0.25$.

5. Conclusions

On the basis of a combined NMR, XAFS, and calorimetric study, it has been possible to determine the local structure of $x PbO/(1 - x)GeO_2$ glasses and shed light on their previously reported complex devitrification mechanisms. In particular, the investigated compositional range can be divided into three regions: (i) $0.00 \leq x \leq 0.05$; (ii) $0.05 < x < 0.25$; (iii) $0.25 \leq x \leq 0.50$. In region i, the system seems to be inhomogeneous because of some nanocrystalline hexagonal GeO_2 dispersed in the glassy matrix. The glass composition gradually changes with the addition of PbO. In region ii, the trend of both T_g and ΔC_p with Pb content strongly indicates that the system remains inhomogeneous with a limiting glass composition of $x \approx 0.25$. In region iii, finally, a complete miscibility was found.

Concerning XAFS evidence on germanium, our measurements showed that most of the Ge ions are in tetrahedral coordination, as in quartz-like GeO_2, whereas for $x \geq 0.10$, an anisotropic distribution of Ge−O bond lengths is seen. Moreover, EXAFS could detect a next nearest neighbor shell attributed to Ge atoms, in agreement with the glass-former role of germanium.

EXAFS and NMR measurements on lead showed that the Pb environment is generally similar to that of crystalline $PbGeO_3$: both trigonal (PbO_3) and tetragonal (PbO_4) groups are present with lead at the apex of oxygen-based pyramids. The $PbGe_3O_7$ crystalline phase has a quite different environment, and this fact can explain the difficulty of this compound to crystallize. On the contrary, the nanoscale separation in zone ii can work as a nucleation agent for the $PbGe_3O_7$ phase.

Acknowledgment. The authors thank the GILDA staff, namely, Dr. Pierlorenzo Solari, for technical and scientific support in performing the XAFS measurements.

References and Notes

(1) Yiannopoulos, Y. D.; Varsamis, C. P. E.; Kamitsos, E. I. *J. Non-Cryst. Solids* **2001**, *293*, 244.
(2) Cox, A. D.; McMillan, P. W. *J. Non-Cryst. Solids* **1981**, *44*, 257.
(3) Murthy, M. K.; Ip, J. *Nature* **1964**, *201*, 285.
(4) Lezal, D.; Pedlíková, J.; Horák, J. *J. Non-Cryst. Solids* **1996**, *196*, 178.
(5) Mailis, S.; Anderson, A. A.; Barrington, S. J.; Brocklesby, W. S.; Greef, R.; Rutt, H. N.; Eason, R. W. *Opt. Lett.* **1998**, *23*, 1751.
(6) Iwasaki, H.; Sugii, K.; Yamada, T.; Nizeki, N. *Appl. Phys. Lett.* **1971**, *18*, 444.
(7) Burns, G.; Scott, B. A. *Phys. Lett.* **1972**, *39A*, 177.
(8) Shashkov, A. Yu.; Efremov, V. A.; Matsichek, I.; Rannev, N. V.; Venevtsev, Yu. N.; Trunov, V. K. *Zh. Neorg. Khim.* **1981**, *26*, 583.
(9) Yue, X.; Mendricks, S.; Hu, Y.; Hesse, H.; Kip, D. *J. Appl. Phys.* **1998**, *83*, 3473 and references therein.
(10) Kip, D.; Mendricks, S.; Moretti, P. *Phys. Status Solidi A* **1998**, *166*, R3.
(11) Ribeiro, S. J. L.; Dexpert-Ghys, J.; Piriou, B.; Mastelaro, V. R. *J. Non-Cryst. Solids* **1993**, *159*, 213.
(12) Umesaki, N.; Brunier, T. M.; Wright, A. C.; Hannon, A. C.; Sinclair, R. N. *Physica* **1995**, *B213-214*, 490.
(13) Červinka, L.; Bergerová, J.; Sigaev, V. N.; Rocca, F. *J. Non-Cryst. Solids* **2001**, *293−295*, 502.
(14) Shelby, J. E. *J. Am. Ceram. Soc.* **1983**, *66*, 414.
(15) Scavini, M.; Tomasi, C.; Speghini, A.; Bettinelli, M. *J. Mater. Synth. Process.* **2001**, *9*, 93.
(16) Fayon, F.; Farnan, I.; Bessada, C.; Coutures, J.; Massiot, D.; Coutures, J. P. *J. Am. Chem. Soc.* **1997**, *119*, 6837.
(17) Fayon, F.; Bessada, C.; Massiot, D.; Farnan, I.; Coutures, J. P. *J. Non-Cryst. Solids* **1998**, *232−234*, 403.
(18) Montagne, L.; Donze, S.; Palavit, G.; Boivin, J. C.; Fayon, F.; Massiot, D.; Grimblot, J.; Gengembre, L. *J. Non-Cryst. Solids* **2001**, *293*, 74 295.
(19) Filipponi, A.; Di Cicco, A.; Natoli, C. R. *Phys. Rev. B* **1995**, *52*, 15122.
(20) Filipponi, A.; Di Cicco, *A. Phys. Rev. B* **1995**, *52*, 15135.
(21) Cargnoni, F.; Bertini, L.; Scavini, M.; Ghigna, P., work in preparation
(22) Leciejewicz, J. *Acta Crystallogr.* **1961**, *14*, 1304.
(23) Nozik, Yu. Z.; Maksimov, B. A.; Fykin, L. E.; Dudarev, V. Ya.; Garashina, L. S.; Gabrielyan, V. T. *Zh. Strukt. Khim.* **1978**, *19*, 731.
(24) Otto, H. H. *Z. Kristallogr.* **1979**, *149*, 197.
(25) Yoko, T.; Tadanaga, K.; Miyaji, F.; Sakka, S. *J. Non-Cryst. Solids* **1992**, *150*, 192.
(26) Topping, J. A.; Harrower, I. T.; Murthy, M. K. *J. Am. Ceram. Soc.* **1974**, *57*, 209.
(27) Napolitano, A.; Macedo, P. B. *J. Res. Nat. Bur. Stand., Sect. A* **1968**, *72* (4), 425.
(28) Lee, S. K.; Tatsumisago, M.; Minami, T. *Phys. Chem. Glasses* **1995**, *36*, 225.
(29) Varshneya, A. K. *Fundamentals of Inorganic Glasses*; Academic Press: Boston, MA, 1994; p 35.